Kinetics and mechanism of the reversible ring-opening of thiamine and related thiazolium ions in aqueous solution

Elizabeth C. Carmichael,[a] Valerie D. Geldart,[a] Robert S. McDonald,*[,a] David B. Moore,[a] Sheila Rose,[a] Lawrence D. Colebrook,[b] Georgia D. Spiropoulos[b] and Oswald S. Tee*[,b]

[a] *Department of Chemistry, Mount St. Vincent University, Halifax, Nova Scotia, Canada B3M 2J6*
[b] *Department of Chemistry and Biochemistry, Concordia University, Montréal, Québec, Canada H3G 1M8*

Kinetic studies of the ring-opening and reclosure reactions of thiamine and three other thiazolium ions (Q^+) in aqueous solution, in the pH range 0–13, have been carried out by stopped-flow and conventional UV–VIS spectrophotometry. At high pH, ring-opening of thiamine exhibits a temporary diversion to the well-known 'yellow form'. Otherwise, the ring-opening reactions are simply first-order in [OH^-], consistent with rate-limiting attack of hydroxide ion at C(2) of the Q^+ ring, producing a pseudobase, T°, which rapidly consumes a second equivalent of hydroxide ion to form the ring-opened enethiolate, ETh^-. In contrast, ring closure of the enethiol in acidic solution exhibits rather complex kinetic behaviour; two processes are observed for most enethiols, including that derived from thiamine. Both the fast process (*a*) and the slower process (*b*) produce the thiazolium ion Q^+ and they exhibit pH- and buffer-independent rate plateaux at low pH. Rapid, repetitive UV spectral scans and NMR spectral studies show that the two processes arise from the independent formation of Q^+ from the two amide rotamers of the enethiol which do not equilibrate under the reaction conditions. The major amide rotamer (~75%) gives rise to the fast process (*a*) and the minor rotamer to the slow reaction (*b*). The pH–rate profile and buffer catalysis studies reveal that the reclosure reaction undergoes a change in rate-limiting step from uncatalysed formation of T° at low pH to its general acid catalysed breakdown at higher pH. The latter process is characterized by a Brønsted α value of 0.70. Additionally, for process (*b*), a general base catalysed pathway for formation of T° can be observed, for which the Brønsted β value is 0.74. The mechanistic details of the ring-opening and reclosure pathways are discussed.

Thiamine (vitamin B_1), or its pyrophosphate, is a cofactor in many enzymatic processes.[1] It contains a quaternary thiazolium ring which is crucial to its catalytic functions,[1,2] and, this ring, like other thiazolium ions, is susceptible to reversible opening in aqueous solution.[3,4] As depicted in Scheme 1, thiazolium ions

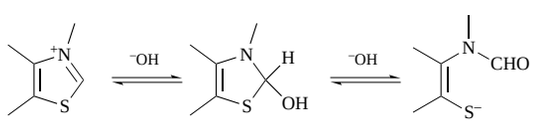

Scheme 1

show a pH-dependent equilibrium which favours the quaternary cation (Q^+) at low pH and a ring-opened enethiolate (ETh^-) at high pH, with a pseudobase[3] (T°) being the most plausible intermediate.[1c,3–9] Even though this type of reaction has been known for a long time,[5] some aspects of the mechanisms involved are still unclear[1c] despite many studies using various kinetic techniques (potentiometry, electrochemistry, pH-stat, stopped-flow and conventional spectrophotometry),[4,7–9] including NMR spectroscopy.[8]

In a previous communication[6c] we reported that two processes occur during the reclosure of the enethiolate (ETh^-) in acidic solution. At the time, we ascribed the faster process to an (N→S) acyl transfer (kinetic control) which precedes the slower reconstitution of the thiazolium ring (thermodynamic control). Other workers have also reported seeing two processes during the reclosure at low pH but they have given different interpretations.[7] Our initial proposal has not been supported by subsequent studies, presented here. It now appears that both the fast and slow processes produce the thiazolium ion, and that they arise because the ring-opened thiolate (and hence the thiol) exists as two rotational isomers[8] which have different propensities for ring closure.

The present results have relevance to the chemistry and biochemistry of thiamine,†[,2] and they may be pertinent to food technology because the vitamin is added to some commercially-prepared foods. The results also relate to the behaviour of tetrahedral intermediates[10,11] since the interconversion of Q^+ and ETh^- almost certainly involves a tetrahedral intermediate T° (Scheme 1) in which nitrogen, oxygen and sulfur are bonded to the pro-acyl carbon. Such species,‡ which are involved in the enzymatic action of thiol proteases as well as other biochemical processes,[1a,12,13] have been studied much less than the more familiar N,O,O- and O,O,O-tetrahedral intermediates.[11]

Results

We first studied the reversible ring-opening of the *N*-methylbenzothiazolium ion (BT^+) and its 2-methyl derivative (MT^+).[5,14,15] The cation BT^+ seemed a good choice for initial

† Several authors[1,2] have speculated that a ring-opened form of thiamine (thiol, thiolate or disulfide) may be transported more easily across cell membranes than thiamine, which is a cation.

‡ For a kinetic study of another reaction involving the intramolecular attack of a thiol on an amide group, and which proceeds through a N,O,S-tetrahedral intermediate, see McDonald *et al.*[12] This reference also has a detailed discussion of related studies of tetrahedral intermediates.

study since it had been studied in some detail by Vorsanger[15] and to a lesser extent by others.[4a,5,14] Also, BT^+ is not subject to the formation of a 'yellow form' which complicates the behaviour of thiamine at high pH.[7a,9] Subsequently, we studied the behaviour of the 3,4-dimethyl-5-(2-hydroxyethyl)thiazolium ion (HET^+) which is a thiamine analogue lacking the pyrimidine moiety and which also has no 'yellow form' in basic solution. Finally, we have carried out studies on thiamine ($B1^+$), itself.

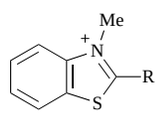

BT^+, R = H
MT^+, R = Me

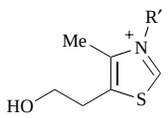

HET^+, R′ = Me
$B1^+$ = Thiamine, R′ =

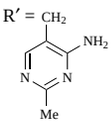

In some pH regions, the kinetics of the ring-opening and reclosure reactions show buffer catalysis. To minimize the contributions of such catalysis to k_{obs}, most experiments were carried out at low buffer concentration (0.01 mol dm^{-3}). For HET^+, where buffer catalysis was studied extensively, the majority of the k_{obs} values used in the pH–rate profiles were the intercepts of buffer plots.

For the overall reaction shown in Scheme 1, it is convenient to employ an equilibrium constant, K_{op}, that is defined [eqn. (1)]

$$K_{op}^2 = [ETh^-][H^+]^2/[Q^+] \quad (1)$$

in such a way that pK_{op} is the pH at which $[Q^+]$ and $[ETh^-]$ are equal.[3] As will be seen below, the pH–rate profiles for opening and reclosure of thiazolium ions go through a minimum at $pH = pK_{op}$.[3,6,7,15] In the vicinity of this pH, the rate constant for equilibration has significant forward and backward components and $k_{obs} = k_{OH}[OH^-] + k_H'[H^+]$. At equilibrium, $k_{OH}[Q^+][OH^-] = k_H'[ETh^-][H^+]$, and so $K_{op}^2 = k_{OH}K_w/k_H'$. Thus, from measured values of k_{OH} and k_H' one can find K_{op}, and in this way Vorsanger[15d] estimated $pK_{op} = 6.57$ for BT^+. Alternatively, K_{op} may be estimated from equilibrium measurements, using various techniques, and Breslow[4a] has found a value of $pK_{op} = 6.35$ for BT^+ by titration with NaOH.

N-Methylbenzothiazolium ion (BT^+)

The pH–rate profile for the opening and reclosure of BT^+ in the pH range 0–12 is shown in Fig. 1. Despite the use of slightly different ionic strengths, there is good agreement between our kinetic results and Vorsanger's,[15] where they meet (Fig. 1), and so we have not duplicated her measurements in the pH region 5–8. For ease of comparison with the other thiazolium ions, the profile is labelled in three parts: process (*a*), ring closure at $pH < pK_{op}$ which becomes the faster process at pH < 4; process (*b*), a slower reclosure at pH < 4; process (*c*), ring-opening at $pH > pK_{op}$. Comparable processes are observable with HET^+ and $B1^+$, as described later.

Above $pH = pK_{op}$, the profile for the ring-opening of BT^+ [Fig. 1(*c*)] rises monotonically to high pH,§ and our data correspond to a rate constant for hydroxide ion attack of $k_{OH} = 7500$ dm^3 mol^{-1} s^{-1} (at $I = 0.1$ mol dm^{-3}), close to Vorsanger's

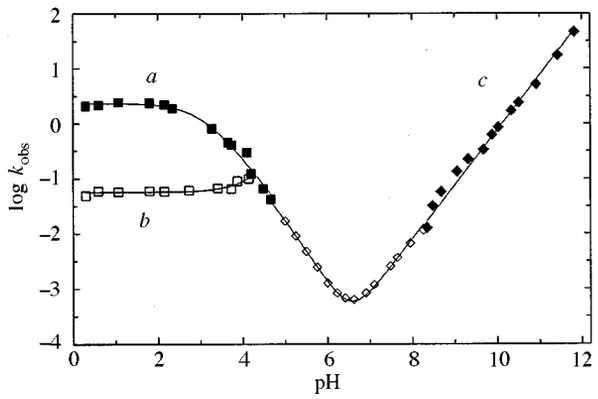

Fig. 1 pH–rate profiles for the ring-opening (pH > 6.5) and reclosure (pH < 6.5) of the *N*-methylbenzothiazolium ion, BT^+, in aqueous solution. The rate constants in the central pH region (◇) are taken (or calculated) from the work of Vorsanger.[15] The other data are from this work: (*a*) = ■, for the reclosure of the major rotamer of the thiol, BTh, which accounts for ~75% of the BT^+ product at low pH; (*b*) = □, for a slower reclosure of the minor rotamer BTh which forms ~25% of BT^+; (*c*) = ◆, for ring-opening of BT^+ to the thiolate, BTh^- (Scheme 2).

value[15b,d] of 8600 dm^3 mol^{-1} s^{-1} (at $I = 0.01$ mol dm^{-3}). The pH–rate profile for the cyclization of BTh^- to BT^+ at $pH < pK_{op}$ shows two significant features: (*i*) a bifurcation into two distinct processes (*a*) and (*b*) near pH 4.2; (*ii*) pH-independent plateaux for both processes at low pH [Fig. 1(*a*) and (*b*)]. On the two plateaux no buffer catalysis is observed but for process (*a*) at pH > 2 there is general acid catalysis, and the buffer plots are curved in a way typical of saturation-type kinetics. Because of the similarity of the two processes between pH 3 and 4, it is not possible to obtain buffer catalysis data of sufficient quality to justify analysis. However, as discussed below for HET^+, these observations are consistent with the break near pH 3 being due to the involvement of an intermediate and a change in rate-limiting step, rather than to a pK_a.

The slower reclosure process (*b*) has a plateau from pH 0–3, after which there is a short rise to meet the profile for process (*a*) at pH 4.2. Such a rise is seen more clearly in the pH–rate profiles for HET^+ and $B1^+$ (see below), and for several other thiazolium ions studied by Knoche and co-workers.[7c]

The UV spectral changes found between pH 5 and 6.5 are as reported by Vorsanger,[15a,c] with BT^+ being the product of reaction. When the pH is lowered from 6.5 to 5, the UV spectrum at time zero alters dramatically since the large absorption maximum of the thiolate BTh^- at 268 nm diminishes with pH [see Fig. 4 in ref. 15(*a*)], corresponding to a pK_a of 5.65[15c] that is attributable to the conjugate acid of BTh^- (BTh, Scheme 2).¶

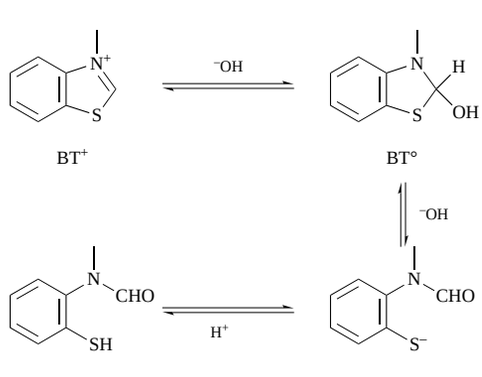

Scheme 2

§ Around pH 9–10, where the data in Fig. 1 tend to deviate above the line defined by the points at higher pH, there is evidence of weak buffer catalysis in borate and carbonate buffers. Such behaviour, which is also observed with HET^+, was anticipated since general base-catalysed attack of water on quaternary heterocyclic cations (and stabilized cations of other types) is well-known.[3] Washabaugh and co-workers[4f,g] have studied such catalysis for various thiazolium ions but ascribe it to general acid catalysed opening of the pseudobase, T°.

¶ Vorsanger[15c] has presented arguments to support attribution of a pK_a of 5.65 to the thiol BTh. In further support, we note that the pK_a of benzenethiol is 6.62, and that electronegative *ortho* substituents lower this to the range 5.4–5.8.[16]

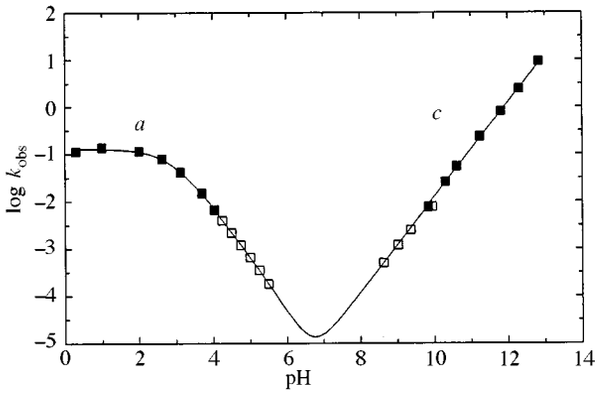

Fig. 2 pH–rate profiles for the ring-opening (pH > 8) and reclosure (pH < 6) of the 2,3-dimethylbenzothiazolium ion, MT^+, in aqueous solution. The open squares (□) are rate constants taken from Vorsanger;[15] the remainder are from this work. The regions are: (*a*) reclosure of the thiol at low pH; (*c*) ring-opening of MT^+ to the thiolate, MTh^-. No process corresponding to (*b*) for the other cations was detected.

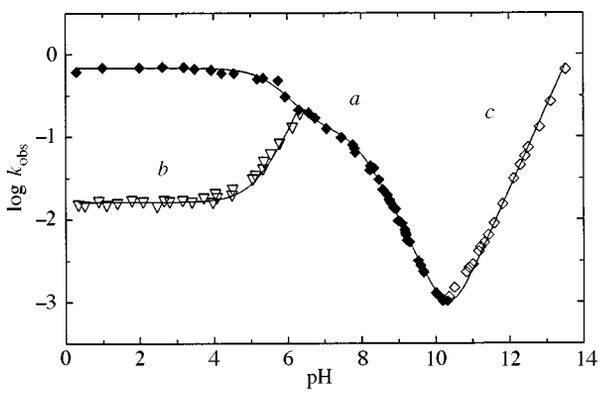

Fig. 3 pH–rate profiles for the ring-opening (pH > 10.3) and reclosure (pH < 10.3) of the cation HET^+. The processes are: (*a*) = ◆, fast ring closure of the major rotamer of HETh to HET^+; (*b*) = ▽, slow ring closure of the minor rotamer of HETh to HET^+; (*c*) = ◇, ring opening of HET^+ to $HETh^-$.

This pK_a does not give rise to a conspicuous break in the pH–rate profile [Fig. 1(*a*)], although Vorsanger detected it in her kinetic data,[15c] and analogous pK_a values are quite evident in the reclosure profiles of HET^+ and $B1^+$ (see later).

2,3-Dimethylbenzothiazolium cation (MT^+)

This cation undergoes ring-opening and reclosure at lower rates than BT^+ (Fig. 2). Again, our kinetic data agree with and extend those of Vorsanger.[15] On the basic side of pK_{op} = 6.75,[15d] the ring-opening of MT^+ continues until high pH, with k_{OH} = 127 dm^3 mol^{-1} s^{-1} for reaction with hydroxide ion. This value is 60-fold lower than that for BT^+, which is attributable to the steric and electronic effects of the methyl group at C(2) and is consistent with simple, rate-limiting hydroxide ion attack on both thiazolium ions.

At pH < pK_{op} the rate profile for the cyclization of the thiolate ion (MTh^-), derived from MT^+, shows a rate increase with acidity that levels off below pH 3. As with BT^+, there is no obvious break in the profile between pH 4 and 6, but Vorsanger[15c] found UV spectral changes at time zero that she ascribed to a thiol pK_a of 5.60. Unlike the situation with BT^+, HET^+, $B1^+$ and other thiazolium ions,[7e] only one kinetic process, labelled (*a*), was observed at low pH.

3,4-Dimethyl-5-(2-hydroxyethyl)thiazolium ion (HET^+)

pH–rate profiles for the reversible hydrolysis of HET^+ have been published,[7e] but it is not clear if the rate constants were corrected for the buffer catalysis present above pH 4. The data we have obtained, corrected for all buffer catalysis, are presented in Fig. 3. Although similar to the profiles for BT^+ (Fig. 1), those for HET^+ are more spread out in the region of ring-closure because pK_{op} = 10.34. Two breaks in the profile for process (*a*) can be clearly seen near pH 6 and 8. As with BT^+, pH-independent fast and slow processes are observed at low pH.

Extensive buffer catalysis studies were carried out for both processes (*a*) and (*b*). Catalysis of process (*a*) is very weak (or non-existent) at pH < 5 and is almost certainly due to a medium effect. A series of phosphate buffers (pH 6.3–7.1) yield saturation-type catalysis plots (Fig. 4) indicative of a reaction through an intermediate and a change in the rate-limiting step. A break in the pH–rate profile near pH 6 also points towards such a change, since the pK_a of the enethiol is expected to be significantly greater than this.[4f,g] Above pH 7.5, formation of the cation HET^+ continues to be strongly buffer catalysed, but the buffer plots are now linear and analysis of their slopes in the usual way reveals that all of the catalysis is general acid catalysis (GAC) in terms of the neutral thiol or a kinetic equivalent.

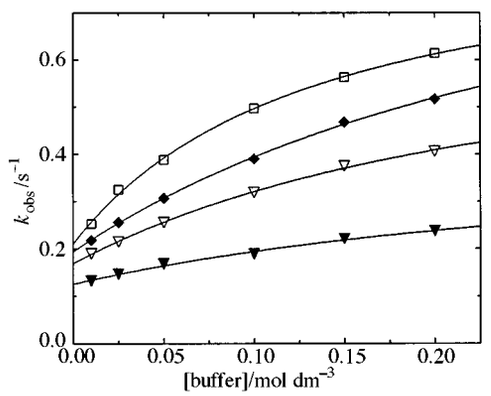

Fig. 4 Curved buffer plots for the ring closure HETh to HET^+. Phosphate buffers of pH 6.31(□), 6.57 (◆), 6.75 (▽), 7.06 (▼). The curves have the form of saturation kinetics, consistent with a change of rate-limiting step.

The second-order rate constants for GAC are collected in Table 1(*a*) and the Brønsted plot with α = 0.70 is illustrated in Fig. 5(*a*).

Between pH 7 and 9 the descending limb of reclosure process (*a*) shows a clear break that can be ascribed to ionization of the enethiol. Analysis of the data on the rate profile in this range allows estimation of the spontaneous (or water catalysed) rate constant for HET^+ formation from neutral thiol, along with its pK_a. For the enethiol, with an acid dissociation constant K_{Th} and a rate constant k_o' for the reaction to give Q^+ [eqn (2)], the

$$ETh^- \underset{K_{Th}}{\overset{[H^+]}{\rightleftharpoons}} ETh \xrightarrow{k_o'} Q^+ \qquad (2)$$

observed rate constant is given by $k_{obs} = k_o'[H^+]/(K_{Th} + [H^+])$. Fitting this equation to the data yields k_o' = 0.127 ± 0.006 s^{-1} and K_{Th} = (1.12 ± 0.06) × 10^{-8} mol dm^{-3} (pK_{Th} = 7.95). When the enethiol is largely ionized (pH > pK_{Th}), $k_{obs} = k_o'[H^+]/K_{Th}$, and so the apparent rate constant for acid catalysis of ring closure of the enethiolate is $k_H' = k_o'/K_{Th}$ = 1.13 × 10^7 dm^3 mol^{-1} s^{-1} as the pH approaches pK_{op}.

Like process (*a*), the slow process (*b*) is independent of pH and [buffer] over the pH range 0–4. At pH > 4, catalysis by hydroxide and by buffers is observed, and the buffer plots are linear. Analysis of the slopes of the buffer plots reveals catalysis that is kinetically general base catalysis (GBC) in terms of the neutral thiol. The second-order rate constants for GBC are also collected in Table 1 and the Brønsted plot (β = 0.74) is shown in Fig. 5(*b*).

In contrast to the rather complex pathways for reclosure, the ring-opening of HET^+ at pH > pK_{op} appears to be straight-

Table 1 Catalytic coefficients for general acid catalysis in process (*a*) and for general base catalysis in process (*b*) for the reclosure of enethiols derived from HET^+ [a]

HA	pK_{HA}	k_{HA}/dm^3 mol^{-1} s^{-1}	k_A/dm^3 mol^{-1} s^{-1}
(*a*) General acid catalysis of process (*a*)			
H_3O^+	−1.74	1.1×10^7	
$H_2PO_4^-$	6.50	8.6 ± 0.4	
N-Me-imidazole (H^+)	7.36	1.6 ± 0.4	
N-Me-morpholine (H^+)	7.77	0.34 ± 0.13	
$(HOCH_2)_3CNH_3^+$	8.34	0.28 ± 0.14	
$HOCH_2CH_2NHMe_2^+$	9.53	0.061 ± 0.021	
H_2O [b]	15.55	2.58×10^{-3}	
(*b*) General base catalysis of process (*b*)			
H_3O^+ [c]	−1.74		2.92×10^{-4}
$ClCH_2CO_2H$	2.66		$(6.5 \pm 0.8) \times 10^{-3}$
HCO_2H	3.41		$(1.95 \pm 0.16) \times 10^{-2}$
CH_3CO_2H	4.52		$(6.8 \pm 3.0) \times 10^{-2}$
$^-O_2CCH_2CO_2H$	5.14		0.10 ± 0.02
$CF_3CH_2NH_3^+$	5.86		1.7 ± 0.2
$MES(H^+)$ [d]	6.27		1.4 ± 0.3
$H_2PO_4^-$	6.50		2.4 ± 0.3
H_2O	15.55		6.4×10^6

[a] At 25.0 °C, $I = 1.00$ mol dm^{-3} (KCl) in H_2O, for which $pK_w = 13.81$. For H_2O, $pK_{HA} = pK_w + \log [H_2O] = 15.55$ and for H_3O^+, $pK_{HA} = -\log [H_2O] = -1.74$. Following common practice, the pK_{HA} values for the buffer acids are taken to be equal to the pH at half-neutralization, in $I = 1.00$ mol dm^{-3} aqueous KCl. [b] Assuming GAC by water, $k_{HA} = 0.143/55.5 = 2.58 \times 10^{-3}$ dm^3 mol^{-1} s^{-1}. More likely, the reaction entails spontaneous ionization. [c] Assuming GBC by water, $k_A = 0.0162/55.5 = 2.92 \times 10^{-4}$ dm^3 mol^{-1} s^{-1}. Possibly, the reaction involves simple attack of water. [d] MES = *N*-morpholinoethanesulfonic acid.

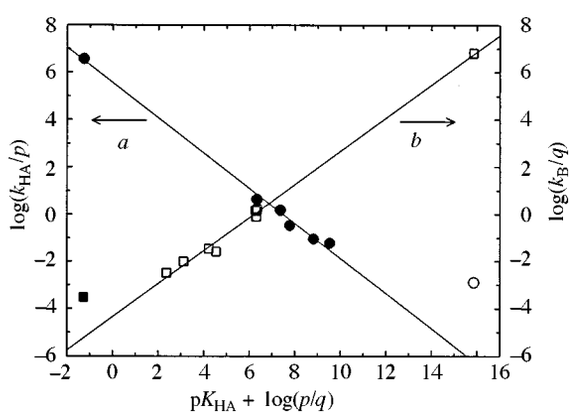

Fig. 5 Brønsted plots for buffer catalysis, constructed from data in Table 1. (*a*) General acid catalysed formation of HET^+ from HETh *via* a pseudobase, HET° [process (*a*)]; the correlation does not include the point for water (○) since it is believed to arise from the spontaneous ionisation of HET°. (*b*) General base catalysed formation of T° from the minor rotamer of HETh [process (*b*)]; the correlation does not include the point for water (■) since it probably represents a different (uncatalysed) mechanism.

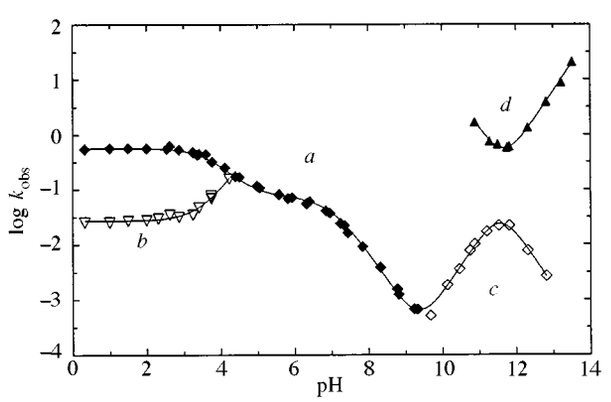

Fig. 6 pH–rate profiles for the ring-opening (pH > 9.5) and reclosure (pH < 9.5) of thiamine ($B1^+$). The processes are: (*a*) = ◆, fast ring closure of the major rotamer of B1Th to $B1^+$; (*b*) = ▽, slow ring closure of the minor rotamer of B1Th to $B1^+$1 (*c*) = ◇, ring opening of the $B1^+$ to $B1Th^-$, after equilibration with YF^-; (*d*) = ▲, equilibration of $B1^+$ with its unstable yellow form, YF^-.

forward. Only one kinetic phase is observed and the pseudo-first-order rate constants are strictly first-order in hydroxide with $k_{OH} = 1.49 \pm 0.08$ dm^3 mol^{-1} s^{-1} ($I = 1.00$ mol dm^{-3}). From this value, with $k_H' = 1.13 \times 10^7$ dm^3 mol^{-1} s^{-1}, (evaluated above), and using $K_{op}^2 = k_{OH}K_w/k_H'$ (derived earlier), one finds $pK_{op} = 10.34$.

In the pH region 10–11, the ring-opening shows no catalysis by *n*-butylamine, triethylamine or 2-(*N*,*N*-dimethylamino)-ethanol buffers. Weak catalysis by carbonate and phosphate buffers was observed but it could not be simply ascribed to a GAC or GBC pathway. Since we could not rule out a specific salt or medium effect of the polyanionic buffer species and because the catalysis is so weak relative to the reaction with hydroxide ion, we did not pursue further study of buffer catalysis in the high pH region.‖

‖ Using iodine trapping of the thiol or thiolate, Washabaugh and co-workers [4f,g] have carried out extensive buffer studies of ring-opening of thiazolium ions at lower pH, where competition from the hydroxide ion is less much important.

Thiamine ($B1^+$)

The pH–rate profiles for the ring-opening and recyclization of thiamine are displayed in Fig. 6. As with BT^+ and HET^+, two processes (*a*) and (*b*) are observed at low pH and process (*a*) continues up to $pH = pK_{op}$. At higher pH, process (*c*), which forms the ring-opened enethiolate, is seen, but at pH > 10 a profile due to a faster process (*d*) appears.

The fast process (*d*) is due to the equilibrium of the cation $B1^+$ with its unstable 'yellow form', YF^- [equilibrium (3)].[6a,7a,9]

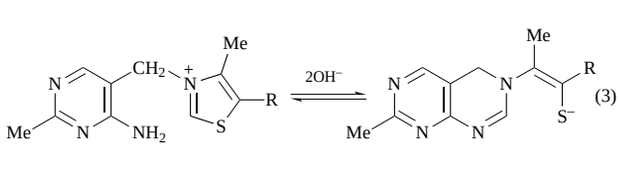

(3)

$B1^+$ (R = CH_2CH_2OH) YF^-

For the equilibrium, a constant is defined by $K_{YF}^2 = [YF^-][H^+]^2/[B1^+]$ which is analogous to K_{op} [eqn. (1)]. Rate constants for the equilibrium have forward and backward components: $k_{obs} = k_f K_w/[H^+] + k_b[H^+]$, and fitting this equation to the

kinetic data gave $k_fK_w = (6.14 \pm 0.19) \times 10^{-13}$ mol dm^{-3} s^{-1} and $k_b = (1.29 \pm 0.6) \times 10^{11}$ dm^3 mol^{-1} s^{-1}, from which $K_{YF} = k_fK_w/k_b^{\ddagger} = (2.18 \pm 0.08) \times 10^{-12}$ mol dm^{-3} and p$K_{YF} = 11.66 \pm 0.02$, close to literature values in the range 11.4–11.6.[6a,7a,9a–c]

The presence of the yellow form, YF^-, in equilibrium with $B1^+$, affects the profile for the ring-opening of thiamine [process (*c*), Fig. 6] and it gives rise to the unusual decrease in k_{obs} at pH > 11.6. Following the original suggestion of Maier and Metzler,[9a] the profile can be accounted for by the steps shown in reaction (4), where B1T° is the pseudobase of thiamine and

$$YF^- \underset{K_{YF}}{\overset{2[H^+]}{\rightleftharpoons}} B1^+ \xrightarrow{k_{OH}[OH^-]} B1T^\circ \overset{OH^-}{\rightleftharpoons} B1Th^- \qquad (4)$$

$B1Th^-$ is its ring-opened enethiolate ion. The corresponding form of k_{obs} is given in eqn. (5), and fitting this equation to the

$$k_{obs} = k_{OH}K_w[H^+]/(K_{YF}^2 + [H^+]^2) \qquad (5)$$

data for process (*c*) gives $k_{OH}K_w = (1.30 \pm 0.05) \times 10^{-13}$ mol dm^{-3} s^{-1} and $K_{YF} = (2.75 \pm 0.10) \times 10^{-12}$ mol dm^{-3}. From these values, $k_{OH} = 8.79 \pm 0.34$ dm^3 mol^{-1} s^{-1} and p$K_{YF} = 11.56 \pm 0.02$, the latter being in reasonable agreement with the values given in the previous paragraph.

The pH–rate profiles for the reformation of thiamine at pH < pK_{op} [Fig. 6(*a*) and (*b*)] are very similar to those of HET^+ (Fig. 3). Moreover, buffer catalysis is observed in the same regions, namely, on the descending limb of process (*a*) and on the rising portion of process (*b*). Also, there is a conspicuous break in process (*a*) near pH 7, and analysis of the kinetic data in the pH range 6.3–8.8, in terms of reaction (2) and in the same way as for HET^+, affords $k_o' = 0.0627 \pm 0.0015$ s^{-1} and $K_{Th} = (7.60 \pm 0.27) \times 10^{-8}$ mol dm^{-3} (p$K_{Th} = 7.12$). Likewise, the rate constant for acid catalysis of ring closure of the thiolate is $k_H' = k_o'/K_{Th} = 8.25 \times 10^5$ dm^3 mol^{-1} s^{-1} in the range pK_{Th} < pH < pK_{op}. Combining this last value with $k_{OH}K_w = 1.30 \times 10^{-13}$ mol dm^{-3} s^{-1} (from above) leads to $K_{op} = (k_{OH}K_w/k_H')^{\ddagger} = 3.97 \times 10^{-10}$ mol dm^{-3} and p$K_{op} = 9.40$, which compares to literature values of pK_{op} of 9.0–9.3.[9]

Rapid UV–VIS spectral studies

The spectral changes we observed by conventional spectrophotometry for the formation and reclosure of the thiolate of BT^+ agreed with those already reported.[14,15] However, using rapid mixing and fast scans, we find that the UV spectral changes for reclosure at pH < 4 have two distinct kinetic phases, corresponding to processes (*a*) and (*b*) in the pH–rate profiles, and both phases are associated with the reformation of the thiazolium ion, as shown below.

Fig. 7(*a*) shows fast repetitive spectral scans recorded during the course of cyclization of the thiolate BTh^- (present as the thiol BTh) at low pH. As is clearly seen in the figure, both the fast and slow kinetic phases lead to increases in the absorption band at 278 nm, and decreases at 250 nm, as expected for the formation of the benzothiazolium cation, BT^+.[14,15] Also, note that the total absorbance change for the faster process is about three times greater than that for the slower process. In a similar way, the spectral changes associated with the reclosures leading to HET^+ and $B1^+$ show two kinetic phases, and the amplitudes of the two phases are also in the ratio of about 3:1 [Fig. 7(*b*) and (*c*)]. By contrast, the ring closure leading to MT^+ shows only one kinetic phase (scans not shown). In all cases the final UV spectrum was identical to that of an appropriate concentration of the relevant cation. These observations have an enlightening correspondence to those made by ^{1}H NMR spectroscopy.

NMR spectral studies

^{1}H NMR studies of thiamine in strongly basic solution have shown the presence of two rotational isomers of the ring-opened thiolate,[4b,8b] arising from slow rotation about the C–N bond of the amide group [equilibrium (6)].**[17] Similarly, we find that two rotamers are formed from the cations BT^+ and HET^+ (Figs. 8–10), and, more significantly, that the ratio of the rotamers is about 3:1 in all three cases (Table 2).

Opening of BT^+ in NaOD–D_2O leads to the 2-(*N*-methylformamido)thiophenolate ion (BTh^-) which displays

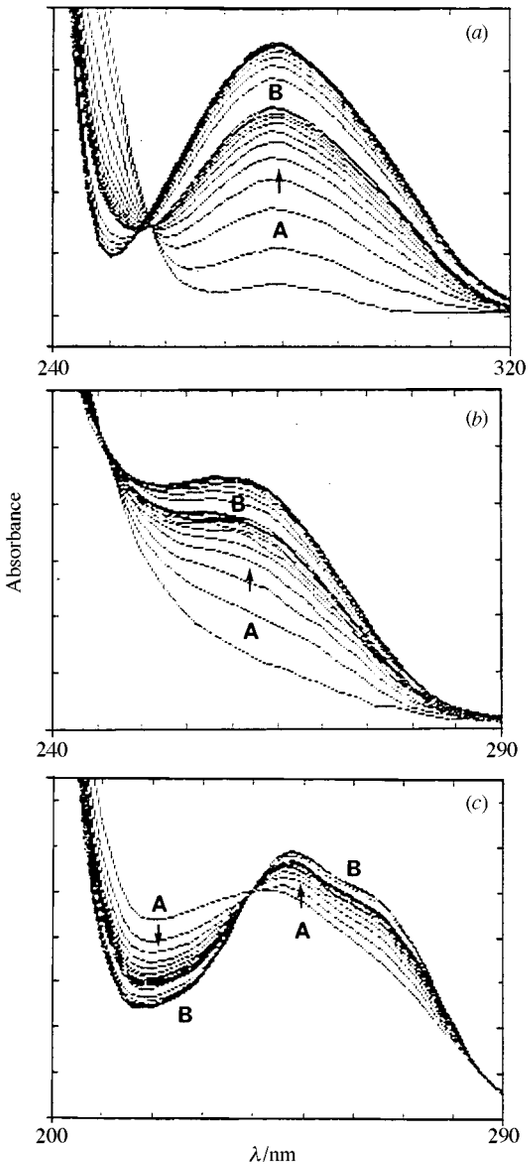

Fig. 7 Rapid UV spectral scans taken during the cyclizations of enethiolates leading to thiazolium ions at low pH. A solution of the enethiolate ion was rapidly quenched with aqueous HCl (see Experimental section). (*a*) Cyclization of the benzenethiol BTh to BT^+; the two time domains are: **A**, 11 scans at 0.2 s/scan; **B**, 13 scans at 10 s/scan. (*b*) Cyclization of the enethiol HETh to HET^+; the two domains are: **A**, 13 scans at 0.5 s/scan; **B**, 13 scans at 20 s/scan. (*c*) Cyclization of the enethiol B1Th to $B1^+$; the two time domains are **A**, 13 scans at 0.5 s/scan; **B**, 6 scans at 20 s/scan.

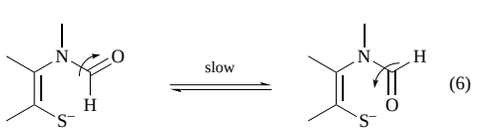

(6)

** In a previous study, from one of our laboratories, two kinetically significant rotamers of *o*-(*N*-methylformamido)-*N*-methylbenzamide were observed by NMR spectroscopy during the course of the opening of the 3,4-dihydro-1,3-dimethyl-4-oxoquinazolinium cation in basic solution.[18] Other examples of reactions involving slowly interconverting amide rotamers are cited in refs. 11(*a*) and 18.

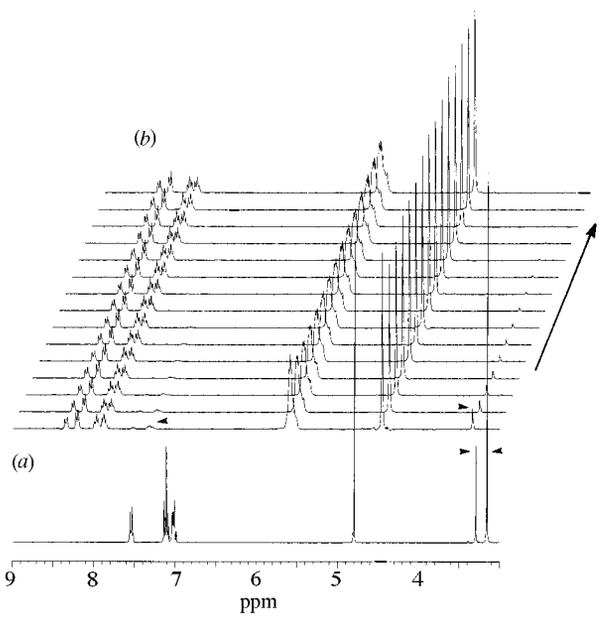

Fig. 8 ^{1}H NMR spectra (300 MHz) taken before and during the cyclization of BTh^- to BT^+. (*a*) Initial ^{1}H NMR spectrum of BTh^- in NaOD–D_2O; note the two *N*-methyl signals for the two amide rotamers. (*b*) Successive single-scan spectra taken at 4 s intervals following acidification with DCl–D_2O. The early traces show a mixture of rapidly formed BT^+ and a small amount of BTh; the latter disappears at the rate of process (*b*).

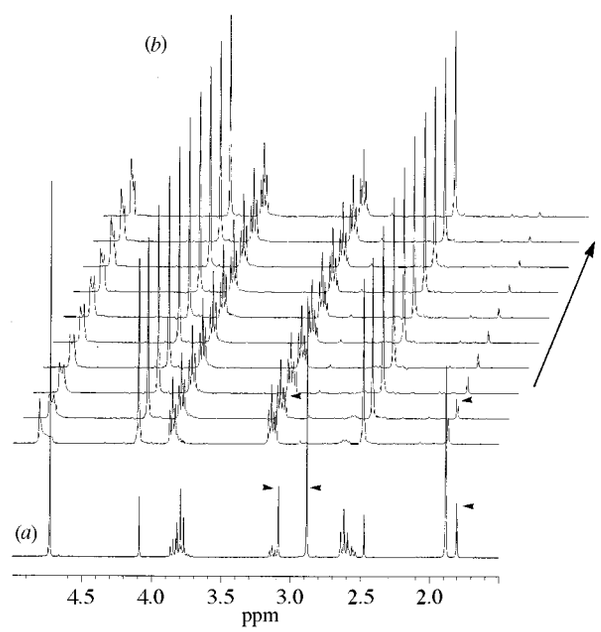

Fig. 9 ^{1}H NMR spectra before and during the cyclization of $HETh^-$ to HET^+. (*a*) Initial ^{1}H NMR spectrum of $HETh^-$ (and some HET^+) in NaOD–D_2O; note the two *C*-methyl signals and the two *N*-methyl signals for the two amide rotamers. (*b*) Successive single-scan spectra taken at 8 s intervals following acidification with DCl–D_2O. The early traces show a mixture of rapidly formed HET^+ and some HETh; the latter disappears at the rate of process (*b*).

two *N*-methyl signals, in the ratio of 3:1 [Fig. 8(*a*)], for the two amide rotamers. When the solution of the thiolate rotamers is quickly acidified with DCl, one of the *N*-methyl signals of the thiol BTh disappears rapidly, as expected for process (*a*) ($t_{\frac{1}{2}} = 0.33$ s), but the other, smaller *N*-methyl signal takes about 1 min, as is appropriate for process (*b*). These NMR observations are consistent with those made by UV spectrophotometry for the two kinetic phases [Fig. 7(*a*)].

When MT^+ is ring-opened to the (*N*-acetylamino)-

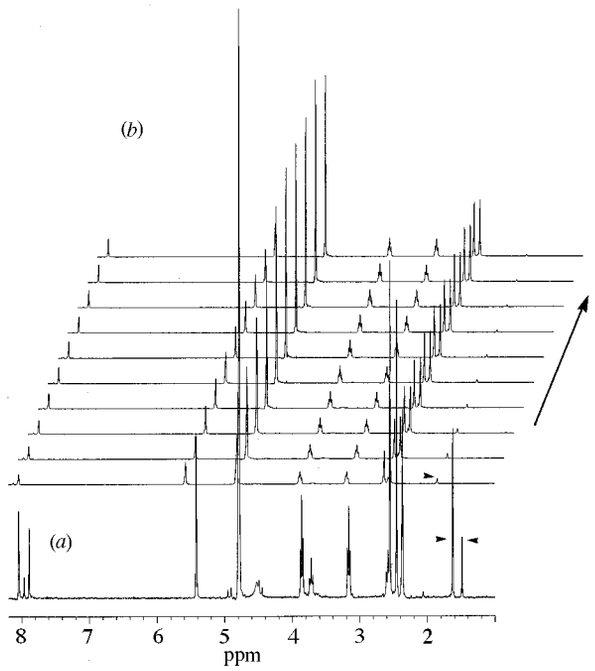

Fig. 10 ^{1}H NMR spectra before and during the cyclization of $B1Th^-$ to $B1T^+$. (*a*) Initial ^{1}H NMR spectrum of $B1Th^-$ (and $B1T^+$) in NaOD–D_2O; note the two *C*-methyl signals for the two amide rotamers. (*b*) Successive single-scan taken at 8 s intervals following acidification with DCl–D_2O. The early traces show a mixture of $B1T^+$ and some B1Th; the latter disappears at the rate of process (*b*).

Table 2 Selected proton NMR spectral data for thiazolium ions and related enethiols and enethiolates[a]

		δ				
Species	Rotamer	*N*-Me	*C*-Me[b]	Other		Major/minor
BT^+		4.46				
BTh^-	Major	3.16				3.1
	Minor	3.30				
BTh	Minor[c]	3.34				
MT^+		4.24	3.17			
MTh^-	Major	3.13	1.81[d]			14.3
	Minor	3.30	~1.75[e]			
HET^+		4.09	2.48	3.13 (t)[f]	3.85 (t)[f]	
$HETh^-$	Major	2.88	1.88	2.61 (t)	~3.79 (t)	3.2
	Minor	3.08	1.80	2.55 (t)	~3.80 (t)	
HETh	Minor[c]	3.11	1.87	~2.65 (t)	~3.85 (t)	
$B1^+$			2.55	2.64[g]	8.03[h]	
$B1Th^-$	Major		1.64	2.39[g]	7.91[h]	3.4
	Minor		1.50	2.40[g]	7.99[h]	
B1Th	Minor[c]		1.86	2.59[g]	8.14[h]	

[a] At 20–25 °C. The cations BT^+, MT^+, HET^+ and $B1^+$ were in D_2O; enethiolates: BTh^-, MTh^-, $HETh^-$ and $B1Th^-$, were in NaOD–D_2O, pD > 10; the corresponding enethiols: BTh, MTh, HETh and B1Th, were obtained by quenching the thiolates with DCl–D_2O, to give pD < 2. The terms 'major' and 'minor' refer to the two amide rotamers of the enethiolates and enethiols. [b] Refers to a methyl group on the thiazolium ion. [c] Major rotamer not observable due to rapid cyclization in the acid medium by process (*a*). [d] Of reduced intensity due to H/D exchange with the medium. [e] Obscured by peaks of the sodium 4,4-dimethyl-4-silapentane-1-sulfonate reference, at δ 1.7–1.8. [f] Methylene protons of the 2-hydroxyethyl group at the 5-position appearing as triplets (t). [g] Methyl group at the 2-position of the pyrimidine ring. [h] Aromatic C–H at the 6-position of the pyrimidine ring.

thiophenolate ion (MTh^-) in basic D_2O and observed by ^{1}H NMR spectroscopy (Table 2), two amide rotamers are observable but they are present in very unequal amounts, in a ratio of about 14:1. So, it is possible that the slow process (*b*) also occurs but it is not easily seen by UV spectrophotometry because its absorbance change is small, only ~6% of that for

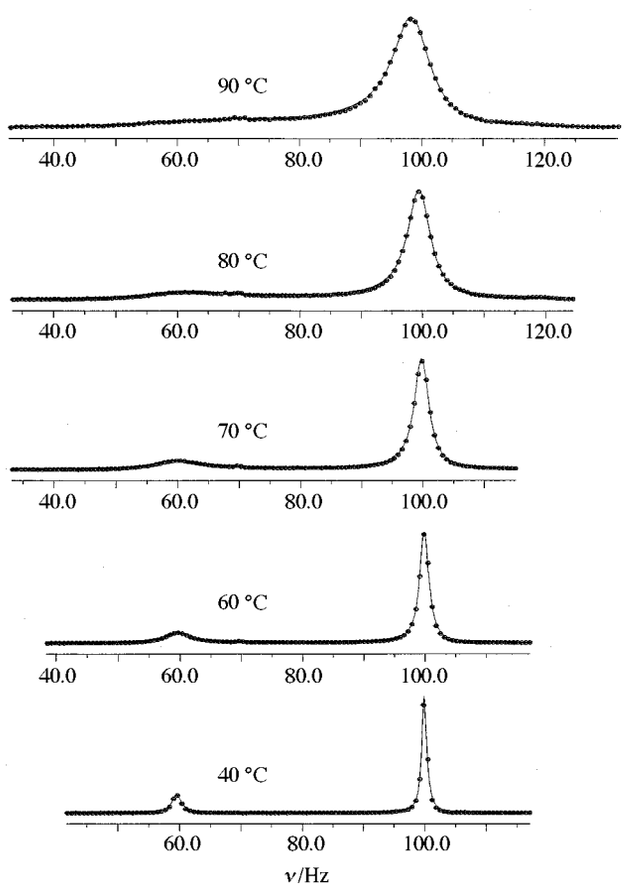

Fig. 11 Digitized experimental (points) and fitted theoretical (smooth curves) spectra showing broadening of the *N*-methyl signals of the two amide rotamers of BTh^- (in $NaOD–D_2O$) over the temperature range 40–90 °C

process (*a*). In addition, it is possible that the two thiol rotamers have fairly similar reactivities, so that their independent closure is not distinct.

The ^1H NMR spectrum of HET^+ in $NaOD–D_2O$ shows two rotamers of the thiolate, $HETh^-$ (Table 2). They are most evident in the *C*-methyl and *N*-methyl signals [Fig. 9(*a*)] and their ratio is 3.2:1. When the thiolate solution is acidified and the thiol cyclizes to the cation HET^+, one of its rotamers disappears rapidly, followed by the slower decay of the other one [Fig. 9(*b*)]. Comparable spectral changes are observed for the opening[4b,8b] and reclosure of thiamine [Fig. 10].

Fitting exponentials to ~20 points for the decaying signals of appropriate *N*-methyl or *C*-methyl groups during the reformation of BT^+, HET^+ and $B1^+$ gave rate constants of 0.065 ± 0.002, 0.015 ± 0.001 and 0.022 ± 0.003 s^{-1} (at 20–25 °C), respectively, in very good agreement with the values of 0.057, 0.016 and 0.029 s^{-1} found for the slow process (*b*) by UV spectrophotometry (at 25 °C). These and the other NMR observations are compatible with those made by UV spectroscopy for the two kinetic phases (Fig. 7). Accordingly, we believe that the faster process (*a*) at low pH in each of the pH–rate profiles (Figs. 1, 3 and 6) is cyclization of the major amide rotamer of the enethiol and that the slower process (*b*) is cyclization of the minor rotamer.

To corroborate the importance of amide rotation, the effect of temperature on the proton spectrum of the benzenethiolate, BTh^-, was also examined. As expected, raising the temperature broadened the NMR signals dramatically (*e.g.* Fig. 11), which is consistent with slow rotation about the N–CO bond at room temperature that is faster at higher temperatures. Mean lifetimes of the two amide rotamers were obtained by complete line shape analysis of the *N*-methyl group signals over the range 40–90 °C (Fig. 11), and from their temperature dependence activation parameters were estimated using linear regression. By extrapolation, free energies of activation ($\Delta G^{\ddagger}$) at 295 K for the major and minor rotamers were estimated to be 78.0 and 75.3 kJ mol^{-1}, respectively, which are in the normal range for amide rotation.[17] The predicted lifetimes of the two rotamers at 295 K are 8.8 and 3.0 s, corresponding to a rate constant of 1.1 s^{-1} for the conversion of the major to the minor rotamer and 3.3 s^{-1} for the reverse. These rate constants are close to that for the faster cyclization [process (*a*)] observed at low pH by UV spectrophotometry and larger than that for the slower one [process (*b*)]. However, it must be realized that the values are not strictly comparable since the NMR results pertain to the thiolate in base, whereas the processes (*a*) and (*b*), seen by UV spectrophotometry, are for the thiol in acidic solution. Nevertheless, the hypothesis that amide rotation may be slow enough to be the origin of the two cyclization processes is supported.

Discussion

Apart from the transient formation of the yellow form (YF^-) from thiamine in base, there are broad similarities between the pH–rate profiles for the thiazolium ions studied: BT^+, MT^+, HET^+ and $B1^+$ (Figs. 1–3 and 6). At $pH > pK_{op}$, ring-opening of the thiazolium ion, Q^+, to the enethiolate, ETh^-, consumes two hydroxide ions (Scheme 1) but the rate of reaction only shows a first-order dependence on $[OH^-]$. This behaviour is evidence for rate-limiting formation of the pseudobase, T°, in equilibrium with ETh^- [reaction (7)].[1c,3,4d,8a] Near $pH = pK_{op}$,

$$Q^+ \underset{k_o}{\overset{k_{OH}[OH^-]}{\rightleftharpoons}} T^\circ \overset{K_2[OH^-]}{\rightleftharpoons} ETh^- \qquad (7)$$

both forward and backward rates are significant, and so the observed rate constant is given by eqn. (8),[8a] which is equivalent

$$k_{obs} = k_{OH}[OH^-] + k_o/K_2[OH^-] \qquad (8)$$

to $k_{obs} = k_{OH}[OH^-] + k_H'[H^+]$, used earlier in the Results section. Note that eqn. (8) is valid only where $pH > pK_{Th}$ and the enethiol exists largely as its anion, ETh^-.

The pH–rate profiles for reclosure at $pH < pK_{op}$ show a region where the rate increases with decreasing pH with a plateau at low pH. In fact, three of the cations, BT^+, HET^+ and $B1^+$, show two processes at low pH, labelled (*a*) and (*b*), both of which have pH-independent plateaux (Figs. 1, 3 and 6).

Biphasic kinetic behaviour during the cyclization of the enethiols has been observed previously.[6b,c,7] European workers attributed the faster process (*a*) to the formation of the pseudobase (T°),[6b,7a] or its *N*-protonated form,[7b,c] and the slower process (*b*) to the breakdown of T° to the thiazolium ion. However, no convincing spectroscopic evidence (UV or NMR) was presented to characterize the proposed intermediate(s). In our previous report,[6c] we suggested that process (*a*) is an *N*- to *S*-acyl transfer that gives an aminothioester, present as its protonated form at low pH. Process (*b*) would then represent conversion of the protonated aminothioester to the cation, Q^+. We had no direct evidence for the thioester intermediate and subsequent spectroscopic studies have failed to find any. Instead, they showed something quite different.

UV spectral studies of the formation of the cations BT^+, HET^+ and $B1^+$ from their respective enethiols at low pH indicate that both kinetic phases lead to the thiazolium ion (Fig. 7) and in each case the absorbance amplitude of the faster process is about three times that of the slower one. In addition, NMR studies show that ring-opening of the three cations gives two slowly interconverting amide rotamers of the corresponding enethiolates (Figs. 8–10) [equilibrium (6)], also in a ratio of about 3:1. This ratio should be more or less maintained when solutions of the enethiolates are rapidly acidified and the rate of equilibration of the two enethiol rotamers should also be slow.[17] Consequently, the fast and slow processes, (*a*) and (*b*), seen at

low pH, are attributed to independent formation of the thiazolium ion (Q^+) from the major and minor amidoenethiol rotamers, respectively. Supporting evidence for this proposal comes from NMR spectra recorded immediately after acidification of enethiolate solutions which reveal that the signals of the major rotamer of the enethiol disappear much more rapidly than those of the minor one, and decay of the latter occurs with a rate constant appropriate to process (*b*).

In keeping with earlier studies on related tetrahedral intermediates,[12,19] we propose that the rate-limiting step on the pH-independent plateaux of the processes (*a*) and (*b*) is the uncatalysed formation of neutral tetrahedral intermediate T° from the two rotamers of the enethiol. In the specific case of HET^+, the break in the pH–rate profile of process (*a*) between pH 5 and 6 (Fig. 3), and the curved buffer catalysis plots (Fig. 4) are indicative of a change in rate-limiting step to the general acid catalysed breakdown of T° to the thiazolium ion, Q^+.†† Only one kinetic process is observed above pH 6.5 and the Brønsted α value of 0.70 found for the buffer catalysis (Table 1) gives no further information about the pathway from T° to Q^+. We propose simply that proton transfer from the general acid to T° is concerted with C–O bond-breaking [equilibrium (9)].‡‡

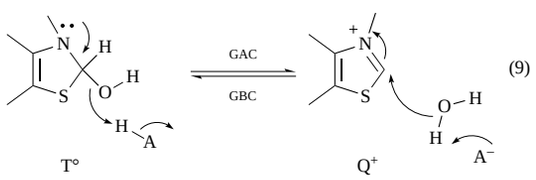

(9)

In contrast to the behaviour of the major rotamer in process (*a*), formation of T° from the minor rotamer in process (*b*) exhibits hydroxide ion catalysis and GBC ($\beta = 0.74$) above pH 4, until the two processes meet near pH 6.5 (in the case of HET^+). We do not observe the analogous base catalysed pathways for the major rotamer since the spontaneous reaction of the enethiol on the plateau of process (*a*) is much faster, and the change in rate-limiting step at pH 5–6 occurs before it can be observed. The buffer catalysis of process (*b*) could represent true GBC of thiol attack on the amide carbonyl, forming the anion of T° which is rapidly protonated [Scheme 3(*a*)], or the

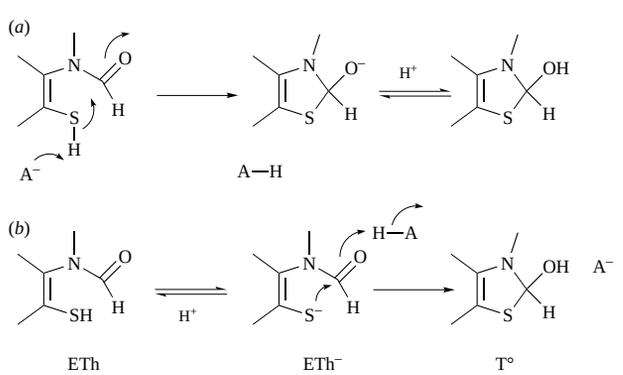

Scheme 3

kinetically-equivalent reaction of GAC of thiolate attack on the amide carbonyl within ETh^- [Scheme 3(*b*)]. Of these two, we favour the latter since a Brønsted α value of 0.26 for such a process is quite reasonable, based on the known behaviour of thiolate ions with carbonyl groups.[20] Also, from a study of irreversible opening of *N*-(*p*-nitrobenzyl)thiazolium ions at pHs near neutrality, achieved by iodine trapping of the thiol and thiolate, Washabaugh and co-workers[4f,g] proposed a GBC-pathway from T° to ETh^- ($\beta = 0.34 \pm 0.05$) and the enethiol ETh, which is the reverse of the GAC-pathway shown in Scheme 3(*b*).

So, for the reclosure reactions at pH < pK_{op}, we believe that breakdown of the pseudobase T° to Q^+ is rate-limiting down to the pH where the plateaux for processes (*a*) and (*b*) are established, at which point formation of T° from the enethiol ETh becomes rate-limiting. In order to account fully for the profiles (*a*), it is necessary to propose conversion of ETh to the intermediate T° which may undergo loss of OH^- spontaneously (k_o) or with proton catalysis (k_2) [reaction (10)], and to make

$$ETh \underset{k_{-1}}{\overset{k_1}{\rightleftharpoons}} T^\circ \xrightarrow[k_2[H^+]]{k_o} Q^+ \qquad (10)$$

allowance for ionization of the thiol at higher pH [equilibrium (11)]. In combination, these processes lead to the expression for

$$ETh \overset{K_{Th}}{\rightleftharpoons} ETh^- + H^+ \qquad (11)$$

k_{obs} given in eqn. (12), assuming that T° is a steady-state intermediate.

$$k_{obs} = \frac{k_1(k_o + k_2[H^+])[H^+]}{(k_1 + k_o + k_2[H^+])(K_{Th} + [H^+])} \qquad (12)$$

Eqn. (12) effectively describes the data for the whole of process (*a*) for the cations BT^+, MT^+, HET^+ and $B1^+$, from pH 0 up to pH = pK_{op}. In the cases of BT^+ and MT^+, ionization of the thiol is not clearly evident in the rate profile (because pK_{Th} is quite close to pK_{op} and k_o is barely significant) and so a simpler version could suffice. The calculated curves for process (*a*) in the rate profiles shown in Figs. 1–3 and 6 were generated with eqn. (12), using parameters given in Table 3.

Where ionization of the enethiol is negligible (pH < pK_{Th}), eqn. (12) reduces to eqn. (13) which describes the plateau of process (*a*) and the pH region just beyond the break. At the lowest pHs, breakdown of the intermediate T° to the cation Q^+ is much faster than its return to enethiol ($k_o + k_2[H^+] \gg k_{-1}$), so that formation of T° is rate-limiting and eqn. (13) simplifies

$$k_{obs} = \frac{k_1(k_o + k_2[H^+])}{(k_1 + k_o + k_2[H^+])} \qquad (13)$$

greatly to $k_{obs} = k_1$, which defines the plateau of process (*a*). As it stands, eqn. (13) is not suitable for fitting to the data because k_{-1} and k_o are not separable.§§ Instead, one must use eqn. (14),

$$k_{obs} = \frac{(k_o'' + k_1[H^+])}{(K_{app} + [H^+])} \qquad (14)$$

in which $k_o'' = k_1k_o/k_2$ and $K_{app} = (k_{-1} + k_o)/k_2$. Note that p$K_{app}$ (= $-\log K_{app}$) corresponds to the break at the end of the plateau and the pH at which the change in the rate-limiting step occurs. Values of pK_{app} are given in Table 3.

In the pH region above pK_{app}, the acidity is sufficiently low that $(k_{-1} + k_o) \gg k_2[H^+]$, and so eqn. (14) reduces to $k_{obs} = (k_o'' + k_1[H^+])/K_{app}$ which describes the pH–rate profile until the ionization of the enethiol intrudes. Without this intrusion, k_{obs} would eventually level off at $k_{obs} = k_o''/K_{app} = k_1k_o/(k_{-1} + k_o) = k_o'$.

To describe the behaviour at pHs between pK_{app} and pK_{op}, while taking account of the ionisation of the enethiol, we impose the inequality $(k_{-1} + k_o) \gg k_2[H^+]$ on eqn. (12), which leads to eqn. (15). A simpler, equivalent form is eqn. (16), which

†† A comparable change in the rate-limiting step has been observed for another reaction involving intramolecular thiol attack on an amide.[12]

‡‡ Obviously this requires that in the reverse direction the attack of water on Q^+ to form T° is general base catalysed, as is suspected (see footnote §).

§§ Also, it turns out that the rate constants k_{-1} and k_o are not very different in magnitude for HET^+ and $B1^+$, but for BT^+ and MT^+ $k_{-1} \gg k_o$ (see later).

Table 3 Rate and equilibrium constants associated with the reversible ring-opening of thiazolium ions (Q^+) in aqueous solution[a]

Process	BT^+	MT^+	HET^+	$B1^+$
k_1/s^{-1} (*a*)	2.3	0.13	0.68	0.57
k_1/s^{-1} (*b*)	0.057	*b*	0.016	0.027
$k_{OH}'/dm^3\ mol^{-1}\ s^{-1}$ (*b*)	2.2×10^8	*b*	6.4×10^6	8.0×10^8
$k_H/dm^3\ mol^{-1}\ s^{-1}$ (*a*)	2400	82	3.3×10^5	3400
$k_H'/dm^3\ mol^{-1}\ s^{-1}$ (*a*)	1830[c]	73[c]	1.1×10^7	8.3×10^5
k_o'/s^{-1} (*a*)	2.2×10^{-3}[c]	9.2×10^{-5}[c]	0.13	0.063
$k_{OH}/dm^3\ mol^{-1}\ s^{-1}$ (*c*)	7500	130	1.5	8.8
k_1/k_o	1040	1400	4.2	8.1
pK_{app}	3.02	2.80	5.69	3.78
pK_{Th}	5.65[c]	5.60[c]	7.95	7.12
pK_{op}	6.57[c]	6.75[c]	10.34	9.40

[a] At 25 °C. The rate constants k_1 correspond to the plateaux of processes (*a*) and (*b*); k_{OH}' is for base catalysis of process (*b*); $k_H = k_1/K_{app}$ is for acid catalysed cyclization of ETh to Q^+, *via* T° [reaction (10)]; $k_H' = k_o'/K_{Th}$ is for the acid catalysed cyclization of ETh^- to Q^+ and k_o' is the related rate constant for the conversion of ETh to Q^+ [reaction (2)]; k_{OH} is for the attack of OH^- on Q^+ to give T° [reaction (7)]; pK_{app} is the pH at the break point of the plateau for process (*a*); pK_{Th} is the thiol pK_a; pK_{op} is the apparent pK_a for the ring-opening [from eqn. (1)]. Since $k_o' = k_1k_o/(k_{-1} + k_o)$, the ratio $k_{-1}/k_o = (k_1/k_o') - 1$. [b] Process (*b*) was not observed. [c] Taken from the work of Vorsanger.[15]

$$k_{obs} = \frac{k_1(k_o + k_2[H^+])[H^+]}{(k_{-1} + k_o)(K_{Th} + [H^+])} \quad (15)$$

$$k_{obs} = \frac{(k_o' + k_H[H^+])[H^+]}{(K_{Th} + [H^+])} \quad (16)$$

is comparable to the equation used earlier by Vorsanger.[15] In eqn. (16), $k_H = k_1k_2/(k_{-1} + k_o) = k_1/K_{app}$ and $k_o' = k_1k_o/(k_{-1} + k_o)$, as above. At the point where $k_2[H^+]$ becomes negligible compared to k_o, the acid catalysed decomposition of T° gives way to its spontaneous ionization, and eqn. (16) reduces further to: $k_{obs} = k_o'[H^+]/(K_{Th} + [H^+])$. This expression was introduced in the Results section to describe the situation depicted in equation (2).

The various equations introduced above were fitted to kinetic data in appropriate regions of pH to arrive at the estimates of the parameters and deduced quantities collected in Table 3. Broadly speaking, the reactivity trends that these parameters show are understandable in terms of the proposed mechanisms. For example, OH^- is less reactive towards MT^+ then BT^+ because of the steric and electronic effects of the 2-methyl group in the former. Likewise, cyclization of the corresponding thiol MTh to MT° is slower than that of BTh to BT° since the former entails nucleophilic attack on a CH_3CO– group whereas the latter involves attack on a HCO– group. As a consequence, pK_{op} for MT^+ and BT^+ are quite similar, since pK_{Th} for the thiols MTh and BTh are very close.

The ratio k_1/k_o measures the tendency of the intermediate T° to ring open to the enethiol ETh, as opposed to losing OH^- to give the cation Q^+. For BT^+ and MT^+, the ratio is 1000–1400, whereas for HET^+ and $B1^+$ the ratio is only 4–8. This large difference probably arises because the thiazolium rings of HET^+ and $B1^+$ are more 'aromatic' than the benzannelated rings of BT^+ and MT^+, so that spontaneous ionization (k_o) is appreciably faster. A less aromatic thiazolium ring can also account for the faster attack of OH^- on BT^+ than HET^+ or $B1^+$ and, together with the easier ionization of the thiol BTh, for the more facile ring-opening (lower pK_{op}) of BT^+.

The reactivity differences between HET^+ and $B1^+$ are attributable to the electron-withdrawing effect of the pyrimidine ring in thiamine. For example, for $B1^+$, k_{OH} is 120 times larger, ring-opening is easier (pK_{op} is lower) and cyclization is slower (see k_H and k_H' in Table 3). It should be noted that thiamine has a $pK_a \approx 4.9$ due to protonation on the pyrimidine ring.[4c,8b,9c] A similar pK_a must exist for B1Th but it is not apparent in the pH–rate profile for cyclization [Fig. 6(*a*)], although it is discernible as a change in the UV spectral amplitude of the process between pH 4 and 5.[9c] Since the state of protonation of the pyrimidine ring of B1Th seems to have little effect on the rate of formation of the thiazolium ring, we have ignored it as we do not believe that it significantly alters the overall mechanistic picture.

Conclusions

The principal conclusions of this paper are that the ring-opening of simple thiazolium ions such as BT^+, HET^+ and $B1^+$ in basic solution produces an amidoenethiolate (ETh^-) that exists as two rotamers, due to slow rotation about the amide N–CO bond, and that these rotamers give rise to two processes upon recyclization at low pH. When a solution of the rotamers of ETh^- is neutralized they are rapidly converted to rotamers of the corresponding enethiol (ETh) which undergoes cyclization through the tetrahedral intermediate, T°. At the lowest pH values, where formation of T° from ETh is rate-limiting, the two rotamers cyclize at different rates, giving rise to two distinct kinetic phases for reconstitution of the corresponding thiazolium ion, Q^+.¶¶

Experimental

Materials

Liquid amines for use in buffer studies were freshly distilled and stored under nitrogen until required. All other buffer components were reagent grade and were used without further purification. Solutions were made up with glass distilled water throughout.

N-Methylbenzothiazolium (BT^+) iodide was made up by a literature procedure.[21] The corresponding methylsulfate was also prepared, as follows. Dimethyl sulfate (7.56 g, 60 mmol) was carefully added to benzothiazole (6.75 g, 50 mmol) in 50 cm^3 of acetone and the mixture was left at room temperature for two days. The resulting off-white crystals were filtered off, washed with diethyl ether and then dried. Yield: 10.8 g (67%). Recrystallized from ether–ethanol, mp 125–127 °C. In D_2O, this material gave the same proton NMR spectrum as the iodide, with an extra peak at δ 3.74 for the $MeSO_4^-$ counter-ion. The iodide and methylsulfate salts of the 2,3-dimethylbenzothiazolium cation (MT^+) were prepared likewise.[15,21]

¶¶ Barrabass *et al.*[7c] attributed the fast process to conversion of the enethiol ETh to the *N*-protonated form (T^+) of T°, and the slow process to conversion of T^+ to the product, Q^+. Based on this attribution, they analysed the pH dependence of the absorbance amplitudes of the fast and slow processes to find pK_a values for ETh and for T^+. For 10 different thiazolium ions, these two pK_a values are similar, if not the same.[7c] According to our interpretation, the two pK_a values should be virtually the same since the two absorbance changes result from reaction of the two rotamers of ETh, in a pH-dependent equilibrium with the two rotamers of the anion, ETh^-.

3,4-Dimethyl-5-(2-hydroxylethyl)thiazolium (HET^+) iodide was initially prepared by methylation of the corresponding thiazole. Later, it was purchased directly from the Aldrich Chemical Company, along with thiamine hydrochloride.

Kinetic methods

All kinetic runs were carried out at 25.0 ± 0.1 °C. Buffer solutions were prepared following normal practice[12,18] and the ionic strengths of the reaction solutions were maintained at 1.00 mol dm^{-3} (KCl or NaCl) or 0.10 mol dm^{-3} (NaCl), as detailed in the main text. Kinetics were followed by monitoring the UV spectral changes associated with the decrease in $[Q^+]$ (or the increase in the enethiolate ion) for ring-opening reactions, and with the increase in $[Q^+]$ for reclosure reactions (*cf.* Fig. 7). The monitoring wavelengths were generally close to maxima to provide large absorbance changes. Slow kinetics ($t_{\frac{1}{2}} > 5$ s) were carried out conventionally using instrumentation and methodology described previously.[12] Fast reactions were studied with a set-up consisting of an Aminco-DW2 spectrophotometer and Aminco-Morrow stopped-flow accessory, with the data acquisition system developed in-house.[18,22] Data analysis followed established practice[22] and for the fast process (*a*) at low pH, which precedes the slower process (*b*), infinity readings were estimated using the Kezdy–Swinbourne method.[23]

For ring-closing reactions, the appropriate thiazolium ion was first opened in a dilute base solution, with three times as much NaOH as cation (0.20–1.00 mmol dm^{-3}). After waiting long enough for the ring-opening to be essentially complete, ring closure was initiated by mixing with an appropriate buffer or acid solution of low pH.

Non-linear fitting of kinetic expressions to pH–rate constant data was performed with computer programs written by one of us and based on the Marquardt algorithm.[24]

Rapid UV spectral scans

These experiments were carried out using a HP 8451A diode array spectrophotometer and a Hi-Tech rapid mixing device. A solution of the enethiolate ion was mixed with dilute acid and the spectral changes accompanying the fast and slow processes (*a*) and (*b*) were monitored in the UV region (Fig. 7). The enethiolate ETh^- was first generated by ring-opening the appropriate cation Q^+ (0.20 mmol dm^{-3}) in aqueous NaOH (2.0 mmol dm^{-3}). The resulting solution of ETh^- was rapidly mixed (1 : 1) with 0.10 mol dm^{-3} aq. HCl, so that initially the reacting solution contained the enethiol (0.10 mmol dm^{-3}) in 0.05 mol dm^{-3} aq. HCl. Timing details are given in the legend of Fig. 7.

The first spectrum recorded is mostly due to the enethiol, ETh, with a small, initial amount of the cation Q^+. As shown in Fig. 7(*a*)–(*c*), for the cations BT^+, HET^+ and $B1^+$, there are two kinetic phases, **A** and **B**, both of which lead to absorbance changes appropriate to the formation of the corresponding cation. In all three cases, the absorbance for **A** are about three times greater than those for **B**, and the timing is such that ~75% of the spectral change occurs during the course of the fast process (*a*) and the remaining ~25% of spectral change spans the slow process (*b*).

NMR studies

^1H NMR spectra were obtained with a Varian Unity INOVA spectrometer, operating at 300 MHz. For acquiring spectra rapidly during the course of cyclization, the spectrometer was run unlocked, without sample spinning, and with all automation disabled. The samples were introduced into the spectrometer as quickly as possible after acidification of the basic solutions in NMR tubes. Following the sample insertion instruction, a single scan was taken for each time in a queued, arrayed delay sequence, which was started as the sample was being lowered into the magnet. Arrayed total delays of 2 and 4 s (recycle times) were employed, the first acquisitions being taken before the sample had stabilized in the probe. Consequently, the first one or two spectra of each data set were discarded.

For the temperature dependence studies, 10 spectra of BTh^- (in NaOD–D_2O, pH > 9) were recorded over the range 40–90 °C. The digitized intensities in the *N*-methyl region were transferred from the spectrometer to another computer for processing. The temperature-dependent spectra (115–145 points) of the *N*-methyl signals were fitted (*e.g.* Fig. 11) in an iterative non-linear regression sequence by the full uncoupled two-site exchange equations of Gutowsky and Holm,[25] using a Simplex algorithm, written in Pascal.[26] The mean lifetimes of the two *N*-methyl group sites, the chemical shift of the major rotamer and the scaling factor were allowed to vary during the fitting sequence; the chemical shift difference between the two *N*-methyl sites, and the linewidth in the absence of exchange were held constant at pre-determined values. An initial estimate of the chemical shift of the major rotamer was made by the software from the input data; starting values for the other parameters in the iterative process were selected by the operator. There was no evidence for any change in the chemical shift difference over the temperature range employed. The HOD signal was used as an internal linewidth reference.

Acknowledgements

This work was made possible by operating and equipment grants from the Natural Sciences and Engineering Research Council of Canada. We also thank Professor Ann English for the use of the diode array spectrophotometer. Some technical assistance was provided by Mr B. K. Takasaki and Mr M. P. Jansen.

References

1 (*a*) C. Walsh, *Enzyme Reaction Mechanisms*, W. H. Freeman, San Fransico, 1979; (*b*) H. Dugas, *Bioorganic Chemistry: A Chemical Approach to Enzyme Action*, Springer-Verlag, New York, 3rd edn., 1989; (*c*) J. A. Zoltewicz and G. Uray, *Biorg. Chem.*, 1994, **22**, 1.

2 (*a*) *Thiamine. Twenty Years of Progress*, eds. H. Z. Sable and C. J. Gubler, N.Y. Acad. Sci., New York, 1982 (*Ann. N.Y. Acad. Sci.*, 1982, **378**, 7–122); (*b*) R. Kluger, *Chem. Rev.*, 1987, **87**, 863; (*c*) P. Haake, in *Enzyme Mechanisms*, ed., M. I. Page and A. Williams, Royal Society of Chemistry, London, 1987.

3 J. W. Bunting, *Adv. Heterocycl. Chem.*, 1979, **25**, 1.

4 (*a*) R. Breslow, *J. Am. Chem. Soc.*, 1958, **80**, 3719; (*b*) Y. Asahi and M. Nagaoka, *Chem. Pharm. Bull. Jpn.*, 1971, **19**, 1017; (*c*) H. Nogami, J. Hasegawa and T. Rikihisa, *Chem. Pharm. Bull. Jpn.*, 1973, **21**, 858; (*d*) J. A. Zoltewicz and G. Uray, *J. Org. Chem.*, 1980, **45**, 2104; (*e*) R. Kluger, J. Chin and T. Smyth, *J. Am. Chem. Soc.*, 1981, **103**, 884; (*f*) M. W. Washabaugh, C. C. Yang, J. T. Stivers and K.-S. Lee, *Bioorg. Chem.*, 1992, **20**, 296; (*g*) M. W. Washabaugh, M. A. Gold and C. C. Yang, *J. Am. Chem. Soc.*, 1995, **117**, 7657.

5 (*a*) W. H. Mills, L. M. Clark and J. A. Aeschlmann, *J. Chem. Soc.*, 1923, 2353; (*b*) L. M. Clark, *J. Chem. Soc.*, 1928, 2313.

6 (*a*) R. F. W. Hopmann, G. P. Brugoni and B. Fol, *J. Am. Chem. Soc.*, 1982, **104**, 1341; (*b*) J. M. El Hage Chahine and J.-E. Dubois, *J. Am. Chem. Soc.*, 1983, **105**, 2355; (*c*) O. S. Tee, G. D. Spiropoulos, R. S. McDonald, V. D. Geldart and D. Moore, *J. Org. Chem.*, 1986, **51**, 2150.

7 (*a*) J. M. El Hage Chahine and J.-E. Dubois, *J. Chem. Soc.*, *Perkin Trans. 2*, 1988, 1409; (*b*) I. Heiber-Langer, I. Winter and W. Knoche, *J. Chem. Soc.*, *Perkin Trans. 2*, 1992, 1551; (*c*) S. Barrabass, I. Heiber-Langer and W. Knoche, *J. Chem. Soc.*, *Perkin Trans. 2*, 1994, 131.

8 (*a*) P. Haake and J. M. Duclos, *Tetrahedron Lett.*, 1970, 461; (*b*) Y. Asahi and E. Mizuta, *Talanta*, 1972, **19**, 567; (*c*) J. M. Duclos and P. Haake, *Biochemistry*, 1974, **13**, 5358.

9 (*a*) G. D. Maier and D. E. Metzler, *J. Am. Chem. Soc.*, 1958, **79**, 4386; (*b*) R. F. W. Hopmann and G. P. Brugoni, *Angew. Chem.*, *Int. Ed. Engl.*, 1981, **20**, 961; (*c*) R. F. W. Hopmann, *Ann. N.Y. Acad. Sci.*, 1982, **378**, 32; (*d*) M. W. Washabaugh, C. C. Yang, A. D. Hollenbach and P. Chen, *Bioorg. Chem.*, 1993, **21**, 170.

10 (*a*) M. L. Bender, *Mechanisms of Homogeneous Catalysis from Protons to Proteins*, Wiley, New York, 1971; (*b*) W. P. Jencks, *Catalysis in Chemistry and Enzymology*, McGraw-Hill, New York, 1968; (*c*) T. H. Lowry and K. S. Richardson, *Mechanism and Theory in Organic Chemistry*, Harper and Row, New York, 3rd edn., 1987.

11 (*a*) B. Capon, A. K. Ghosh and D. M. A. Grieve, *Acc. Chem. Res.*, 1981, **14**, 306; (*b*) J. P. Guthrie, *Acc. Chem. Res.*, 1983, **16**, 122; (*c*) R. A. McClelland and L. J. Santry, *Acc. Chem. Res.*, 1983, **16**, 394.
12 R. S. McDonald, P. Patterson and A. Stevens-Whalley, *Can. J. Chem.*, 1983, **61**, 1846.
13 A. Fersht, *Enzyme Structure and Mechanism*, W. H. Freeman, Reading, 2nd edn., 1985.
14 J. Metzger, H. Larivé, R. Dennilauler, R. Baralle and C. Gaurat, *Bull. Soc. Chim. Fr.*, 1964, 2868.
15 (*a*) H. Vorsanger, *Bull. Soc. Chim. Fr.*, 1964, 3118; (*b*) H. Vorsanger, *Bull. Soc. Chim. Fr.*, 1967, 551; (*c*) H. Vorsanger, *Bull. Soc. Chim. Fr.*, 1967, 556; (*d*) H. Vorsanger, *Bull. Soc. Chim. Fr.*, 1967, 2124.
16 P. De Maria, A. Fini and F. M. Hall, *J. Chem. Soc.*, *Perkin Trans. 2*, 1974, 1443.
17 (*a*) G. Binsch, *Top. Stereochem.*, 1968, **3**, 132; (*b*) R. L. Stein, *Adv. Protein Chem.*, 1993, **44**, 1; (*c*) E. L. Eliel and S. H. Wilen, *Stereochemistry of Organic Compounds*, Wiley, New York, 1994, pp. 553–555; (*d*) Cf. C. Cox, D. Ferraris, N. N. Murthy and T. Lectka, *J. Am. Chem. Soc.*, 1996, **118**, 5332.
18 O. S. Tee, M. Trani, R. A. McClelland and N. E. Seaman, *J. Am. Chem. Soc.*, 1982, **104**, 7219.
19 (*a*) A. J. Kirby and P. W. Lancaster, *J. Chem. Soc.*, *Perkin Trans. 2*, 1972, 1206; (*b*) M. F. Aldersley, A. J. Kirby, P. W. Lancaster, R. S. McDonald and C. R. Smith, *J. Chem. Soc.*, *Perkin Trans. 2*, 1974, 1487; (*c*) A. J. Kirby, R. S. McDonald and C. R. Smith, *J. Chem. Soc.*, *Perkin Trans. 2*, 1974, 1495; (*d*) M. F. Aldersley, A. J. Kirby and P. W. Lancaster, *J. Chem. Soc.*, *Perkin Trans. 2*, 1974, 1504; (*e*) T. H. Fife and Duddy, *J. Am. Chem. Soc.*, 1983, **105**, 74.
20 W. P. Jencks and H. F. Gilbert, *Pure Appl. Chem.*, 1977, **49**, 1021.
21 H. Wahl and M. T. Le Bris, *Bull. Soc. Chim. Fr.*, 1959, 343.
22 O. S. Tee and B. K. Takasaki, *Can. J. Chem.*, 1985, **63**, 3540.
23 E. S. Swinbourne, *Analysis of Kinetic Data*, Nelson, London, 1971.
24 P. R. Bevington, *Data Reduction and Error Analysis for the Physical Sciences*, McGraw-Hill, New-York, 1969; D. M. Bates and D. G. Watts, *Nonlinear Regression Analysis and its Applications*, Wiley, New York, 1988; L. M. Mezei, *Practical Spreadsheet Statistics and Curve Fitting for Scientists and Engineers*, Prentice-Hall, Englewood Cliffs, New Jersey, 1990.
25 H. S. Gutowsky and C. H. Holm, *J. Chem. Phys.*, 1956, **25**, 1228.
26 M. S. Caceci and W. P. Cacheris, *Byte*, 1986, **9**, 340.

Paper 7/05143C
Received 17*th July* 1997
Accepted 28*th August* 1997